THE JOURNAL OF PHYSICAL CHEMISTRY C

Article

pubs.acs.org/JPCC

Thickness Effects on Light Absorption and Scattering for Nanoparticles in the Shape of Hollow Spheres

Jeng-Yi Lee,[†] Min-Chiao Tsai,[‡] Po-Chin Chen,[‡] Ting-Ting Chen,[‡] Kuei-Lin Chan,[‡] Chi-Young Lee,[‡] and Ray-Kuang Lee*[,†,§]

[†]Institute of Photonics Technologies, [‡]Department of Materials Science and Engineering, and [§]Frontier Research Center on Fundamental and Applied Sciences of Matters, National Tsing-Hua University, Hsinchu 300, Taiwan

ABSTRACT: We reveal the thickness effects on optical properties for nanoparticles in the shape of hollow spheres theoretically and experimentally. Within and beyond the electrically small limit, hollow spheres are shown to have almost the same light absorption power as that of solid ones, when the ratio of inner core to whole particle radii is smaller than 0.4. It means that one can maintain the level of light absorption even with a large empty core. In the electrically small limit, we expand the exact solution of Mie theory in power of the thickness parameter and show that the thickness ratio has less influence on light absorption. Moreover, we synthesize highly uniform hollow spheres of TiO_2 anatase through a self-sacrificing template method. A variety of particle radii from 94 to 500 nm, with 50 nm in the shell thickness, are performed experimentally in photocatalytic activity. With experimental demonstrations and theoretical simulations, our results provide a guideline in the design on the thickness for hollow-sphere nanoparticles with an optimized absorption power in light harvesting.

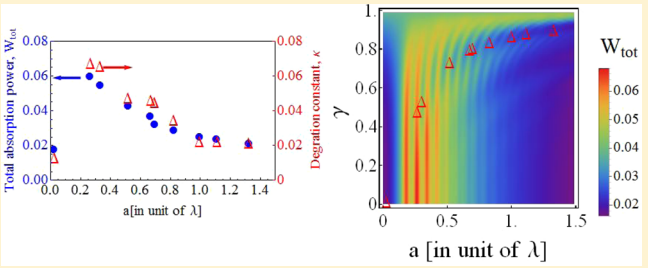

INTRODUCTION

Photocatalyst has acted as one of solutions to utilize solar light into available energy, with environmental friendly and highly efficient materials synthesized for water splitting, CO_2 reduction, and green energy applications.[1,2] In particular, TiO_2 is the major photocatalyst to decompose water into hydrogen and oxygen and used as a clean and recyclable energy source for hydrogen fuel.[3−5] It is known that TiO_2 has the energy gap about 3.2 eV, and when excited by a UV−visible light source, a pair of electron and hole is generated. Consequently, this excited electron−hole pair migrates to the surface to serve as electron donor and acceptor, resulting in the photocatalytic reaction. Based on this series of electrochemical reactions, several methods are demonstrated to enhance the photocatalytic activity with TiO_2. For example, to reduce the recombination of separated electron−hole pairs, one can blend various TiO_2 phases, deposit metal materials on the surface, or introduce trapping sites to inhibit the recombination.[6−8] As the aim to extend absorption regime in TiO_2 to visible wavelength, doping specific metal or nonmetal elements are demonstrated for light harvesting.[9−14]

Instead of chemical or material approaches mentioned above, intricate structure and morphology can exhibit fascinating properties to improve photocatalytic activity.[15−19] Inspired by materials in nature, like seashells and plant seeds, an alternative way to enhance photocatalytic performance is utilizing nanosized TiO_2 particles.[15] As a rule of thumb, the exposure surface area grows when the size of particles decreases. For light absorption and scattering, it is known that resonance effect emerges as the size of the nanoparticle approaches the wavelength of incident light, known as Mie's scattering effect.[20] Recently, size-dependent Mie's scattering effect with TiO_2 nanoparticles is reported for a superior photoactivity of H_2 evolution.[15,16] In addition to synthesizing different geometrical sizes, nanoparticles can also be formed in the shape of hollow spheres, which have been widely used as adsorbents, delivery carriers, catalysts, and biomedical detectors.[17−19,21] Even though enhancement in photocatalytic function by a variety of geometrical structures has been demonstrated, a systematic investigation to understand the thickness effect on light absorption for nanoparticles in the shape of hollow spheres is still needed to provide a guideline to design optimized core−shell structures for light harvesting.

By taking the complicated photoelectrochemical reaction as a pure optical problem, in this work, we study optical response of incoherent hollow spheres with different geometrical and material parameters based on the exact solutions of Mie's scattering theory. Analytically, we derive the formula for light absorption and scattering coefficients by expanding the thickness parameter. Our theoretical results not only give good agreement to the numerical solutions conducted from Mie theory, but also reveal a counterintuitive scattering property of hollow spheres. We find that as long as the thickness ratio, that is, the ratio of inner core radius to whole particle radius is smaller than a critical value, about 0.4, an individual hollow sphere is shown to have almost the same light

Received: August 30, 2015
Revised: October 16, 2015
Published: October 23, 2015

DOI: 10.1021/acs.jpcc.5b08435
J. Phys. Chem. C 2015, 119, 25754−25760

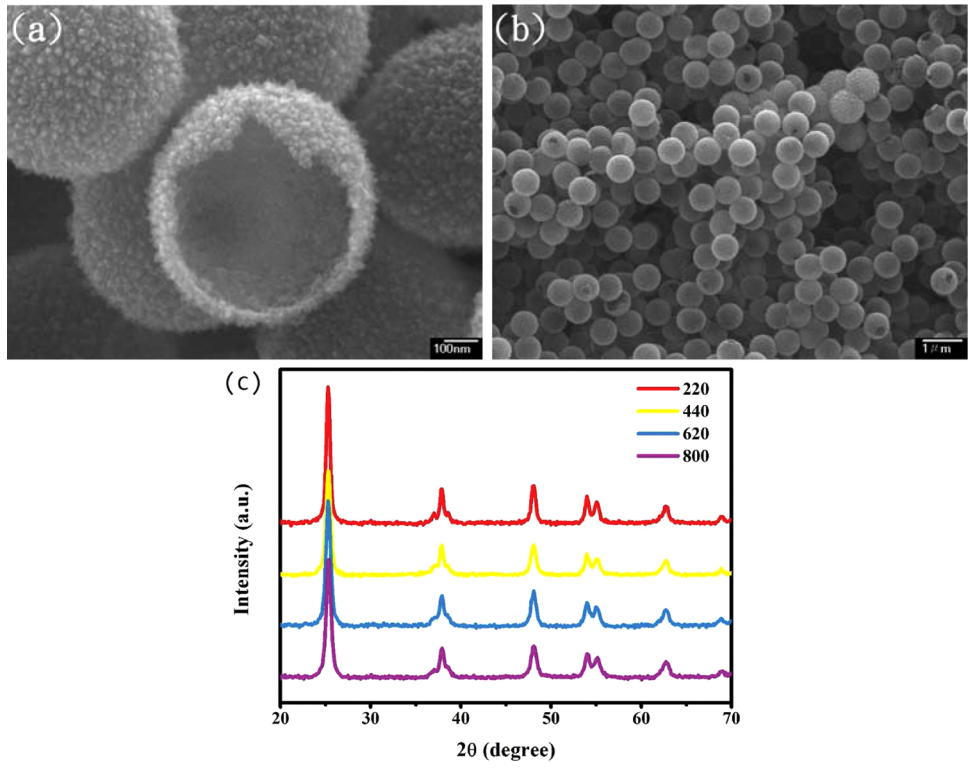

Figure 1. (a, b) SEM images at various magnifications of TiO_2 nanoparticles in the shape of hollow spheres. (c) XRD spectra of our hollow-sphere nanoparticles, shown in different diameters.

absorption as a solid one. In contrast to the naive picture, with a different thickness parameter, one can also have a higher total absorption power for a larger particle size. Moreover, we perform experimentally the photocatalytic activity by synthesizing highly uniform hollow spheres of amorphous TiO_2 anatase through a self-sacrificing template method. With the measurements on photodegradation of methylene blue, thickness effect on a variety of particle radii from 94 to 500 nm is studied experimentally for light absorption. With experimental demonstrations and theoretical simulations, our results provide recipes to design highly efficient photocatalysis with benefits from reducing volume of material use.

MIE THEORY FOR HOLLOW-SPHERE NANOPARTICLES

Before giving the theoretical model for nanoparticles in the shape of hollow spheres, we briefly describe our synthesis method. Typical scanning electron microscope (SEM) images of our TiO_2 hollow-sphere nanoparticles are shown in Figure 1a,b, with different particle radii. These TiO_2 nanoparticles are synthesized using titanium isopropoxide (TTIP, 97%, Aldrich), valeric (99%), and butyric (99.5%) acids in anhydride alcohol (99.5%). Our synthesis process can be viewed as a two-stage transformation. First, the amorphous TiO_2 reacts with F^- ions in the NaF solution to form H_2TiF_6, resulting in dissolving and shrinking in particle size. Then, in the second stage, nanocrystalline particles grow slowly into the shape of hollow spheres, composed of rhomboid anatase. By controlling the concentration of NaF solution, we can synthesize TiO_2 nanoparticles in different sizes, while the concentration of the F^- ion modifies the thickness of hollow spheres. As shown in Figure 1, highly uniform TiO_2 nanoparticles in the shape of hollow spheres are demonstrated with the radius varying from 94 to 500 nm. The resulting thickness for the shell region is also tunable, from 50 to 100 nm.

X-ray diffraction (XRD) measurement (Bruker D8-advanced with Cu Kα radiation λ = 1.5405981 Å) is applied to characterize the crystal structure of our hollow-sphere nanoparticles, as shown in Figure 1c for diameters in 220, 440, 620, and 800 nm, respectively. By using Scherrer's formula, our XRD spectra reveal the corresponding grain size with 14.6, 13.2, 13.1, and 12.6 nm, respectively. As shown in XRD patterns, highly uniform crystallinity of various-sized TiO_2 nanoparticles in the shape of hollow spheres is demonstrated. The results show that the crystallinity for all samples are the same. More details on the method to prepare amorphous precursor spheres can be found in our previous work.[17,18] Due to its superior photocatalytic performance, we use this TiO_2 anatase as our studying materials.

To identify the difference between optical responses from solid-sphere and hollow-sphere nanoparticles, we consider an incident plane wave on a spherical object, as illustrated in Figure 2. This sphere has a bilayer structure, denoted as the core and shell regions. The inner radius of core is denoted as a_c; while the outer radius of whole particle is denoted as a. Material properties are characterized by the permittivity ϵ_i and permeability μ_i, where i = e, s, or c that denotes the environment, shell, and core regions, respectively. Without loss of generalities, the particle is embedded inside a lossless material. All materials are taken as nonmagnetic ones, that is, $\mu_e = \mu_s = \mu_c = 1$. In the following, we use prime and double prime to denote the real and imaginary parts of the dielectric function, that is, $\epsilon = \epsilon' + i\epsilon''$. Moreover, corresponding to the photocatalytic experiment carried out later, we set our background environment as water, with a constant dielectric function in the UV–visible region $\epsilon_e = 1.77$. We also assume

DOI: 10.1021/acs.jpcc.5b08435
J. Phys. Chem. C 2015, 119, 25754–25760

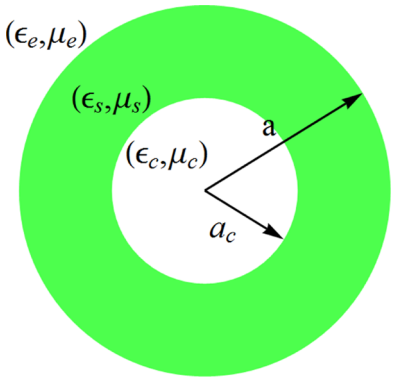

Figure 2. Schematic of a hollow sphere in the core−shell configuration. The corresponding wavenumbers for each region are defined as $k_e = \sqrt{\mu_e\epsilon_e}k_0$, $k_s = \sqrt{\mu_s\epsilon_s}k_0$, and $k_c = \sqrt{\mu_c\epsilon_c}k_0$ for the environment, shell, and core, respectively, where $k_0 \equiv 2\pi/\lambda$ is the wavenumber in the vacuum with the wavelength denoted by λ.

that the core region is filled with water. It is known that TiO_2 anatase is also a birefringence material. However, due to the random distribution of TiO_2 nanoparticles in water, one can safely ignore such an optical anisotropy property. The optical dielectric function within UV−visible light spectra for TiO_2 nanoparticles, in particular, for the wavelength λ = 388 nm (corresponding to 3.2 eV band gap energy), is around $6.25 < \epsilon' < 10$ for the real part and $0 < \epsilon'' < 0.5$ for the imaginary part.[22,23] In the following, we also take the complex dielectric constant into the calculations, with applications in the photocatalytic process.

Now, an x-polarized electric plane wave (incident wave) is assumed to propagate along the z direction with the time dependence $e^{-i\omega t}$, where ω is the angular frequency. Based on Mie theory,[24] the scattering electric and magnetic fields can be generated through two auxiliary vector potentials, only with radial components in the spherical coordinate. These two auxiliary vector potentials are $\vec{A}_{scat}$ (magnetic vector potential) and $\vec{F}_{scat}$ (electric vector potential), which can be decomposed into two infinite series of complex scattering coefficients S_n^{TM} and S_n^{TE}, with the subscript to denote n-th order spherical harmonic channel. These complex scattering coefficients, S_n^{TM} and S_n^{TE}, can be determined by the boundary conditions of each layer, due to the continuity of magnetic and electric fields along the spherical surface. The complex scattering coefficients, S_n^{TM} and S_n^{TE}, can be recast in the following compact forms:[24]

$$S_n^{TE} = -\frac{1}{1 + i(V_n^{TE}/U_n^{TE})} \tag{1}$$

$$S_n^{TM} = -\frac{1}{1 + i(V_n^{TM}/U_n^{TM})} \tag{2}$$

where

$$U_n^{TM} = \begin{vmatrix} j_n(k_c a_c) & j_n(k_s a_c) & y_n(k_s a_c) & 0 \\ \frac{1}{\epsilon_c}[k_c a j_n(k_c a_c)]' & \frac{1}{\epsilon_s}[k_s a j_n(k_s a_c)]' & \frac{1}{\epsilon_s}[k_s a y_n(k_s a_c)]' & 0 \\ 0 & j_n(k_s a) & y_n(k_s a) & j_n(k_e a) \\ 0 & \frac{1}{\epsilon_s}[k_s a j_n(k_s a)]' & \frac{1}{\epsilon_s}[k_s a y_n(k_s a)]' & \frac{1}{\epsilon_e}[k_e a j_n(k_e a)]' \end{vmatrix} \tag{3}$$

and

$$V_n^{TM} = \begin{vmatrix} j_n(k_c a_c) & j_n(k_s a_c) & y_n(k_s a_c) & 0 \\ \frac{1}{\epsilon_c}[k_c a j_n(k_c a_c)]' & \frac{1}{\epsilon_s}[k_s a j_n(k_s a_c)]' & \frac{1}{\epsilon_s}[k_s a y_n(k_s a_c)]' & 0 \\ 0 & j_n(k_s a) & y_n(k_s a) & y_n(k_e a) \\ 0 & \frac{1}{\epsilon_s}[k_s a j_n(k_s a)]' & \frac{1}{\epsilon_s}[k_s a y_n(k_s a)]' & \frac{1}{\epsilon_e}[k_e a y_n(k_e a)]' \end{vmatrix} \tag{4}$$

Here, both V_n and U_n are 4 × 4 determinants, $j_n(.)$ is the corresponding spherical Bessel function, $y_n(.)$ is the corresponding spherical Neumann function, $[xj_n(x)\ ]'$ represents $\frac{d}{dx}[xj_n(x)]$, and $[xy_n(x)\ ]'$ represents $\frac{d}{dx}[xy_n(x)]$, respectively. Eqs 1−4) show the exact formulas of Mie's scattering theory for a core−shell sphere with isotropic and homogeneous permittivities and permeabilities in each layer. These equations are also given in a symmetric form, that is, the formulas for U_n^{TM} (V_n^{TM}) and U_n^{TE} (V_n^{TE}) have similar mathematical forms but with slight differences on physical parameters (just replacing dielectric constant ϵ by permeability μ).

To give a quantitative analysis, we define the quantity to measure how much amount of power is absorbed by a nanoparticle, that is, the absorption cross section Q_{abs},

$$Q_{abs} = \frac{W_{abs}}{I_{inc}} = Q_{ext} - Q_{scat} \tag{5}$$

where I_{inc} is the intensity of incident wave in the unit of power per unit area. The corresponding extinction cross section and scattering cross section, dented as Q_{ext} and Q_{scat}, have the forms:

$$Q_{scat} = \frac{W_{scat}}{I_{inc}} = \frac{2\pi}{|k_e|^2}\sum_{n=1}^{\infty}(2n+1)(|S_n^{TE}|^2 + |S_n^{TM}|^2) \tag{6}$$

$$Q_{ext} = \frac{W_{ext}}{I_{inc}} = -\frac{2\pi}{|k_e|^2}\sum_{n=1}^{\infty}(2n+1)\mathrm{Re}\{S_n^{TE} + S_n^{TM}\} \tag{7}$$

Here, W_{abs}, W_{scat}, and W_{ext} correspond to the absorption, scattering, and extinction powers, respectively. Even though above results are a consequence of Mie theory, it is too general to have a clear physical picture on the thickness effect for hollow spheres. Below we expand the thickness parameter to give analytical formulas.

Electrically Small Limit. First of all, as the size parameter a/λ in each layer is small enough, satisfying the condition $k_e a \ll 1$ and $k_s a \ll 1$, we have analytic formulas for the corresponding cross sections. In this electrically small limit, one can approximate the spherical special functions by a series of polynomial functions, that is, $j_n(x) \approx \frac{2^n n!}{(2n+1)!}x^n$ and $y_n \approx -\frac{(2n)!}{2^n n!}x^{-n-1}$. With this series expansion, we can expand the complex scattering coefficients S_n^{TM} and S_n^{TE} shown in eqs 3 and 4 into

$$U_n^{TM} \approx -\frac{1}{2n+1}\left[\frac{2^n n!}{(2n+1)!}\right]^2\left(\frac{k_c}{k_e}\right)^n\left(\frac{k_e}{k_s}\right)(k_e a)^{2n-1}(n+1)\epsilon_s^{-2}\epsilon_e^{-1}\epsilon_c^{-1} \times \{(\epsilon_c - \epsilon_s)\gamma^{2n}[(n+1)\times\epsilon_s + n\epsilon_e] + \gamma^{-1}(\epsilon_s - \epsilon_e) \times [n\epsilon_c + (n+1)\epsilon_s]\} \tag{8}$$

DOI: 10.1021/acs.jpcc.5b08435
J. Phys. Chem. C 2015, 119, 25754−25760

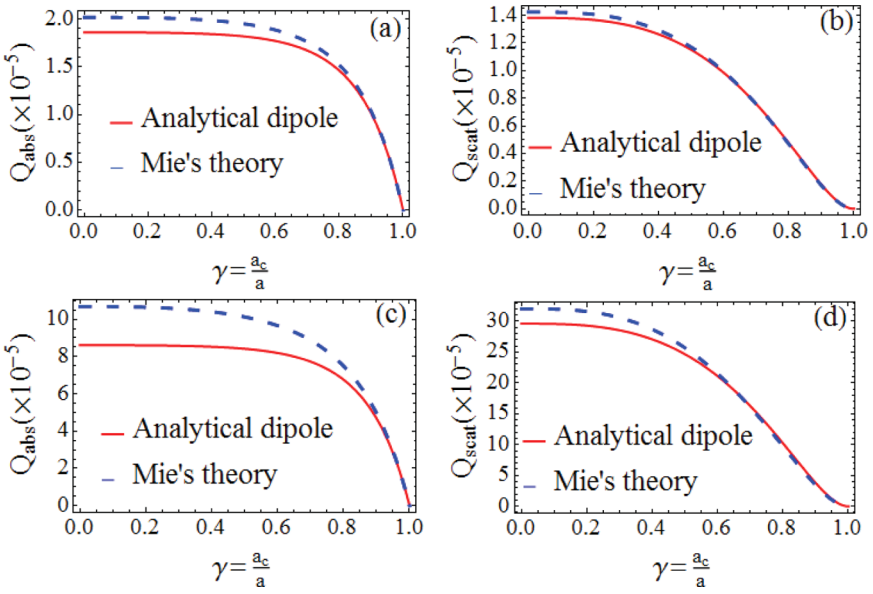

Figure 3. Absorption cross section Q_{abs} and scattering cross section Q_{scat} for nanoparticles in the shape of hollow spheres are shown as a function of the thickness ratio, $\gamma = \frac{a_c}{a}$. Analytical equations shown in eqs 10 and 11 based on the dynamic dipole limit and numerical solutions by Mie's exact solutions are depicted in solid and dashed curves, respectively. Here, the dielectric constant in the shell region is set as $\epsilon_s = 7 + 0.1i$, and the dielectric constants for environment and core regions are $\epsilon_e = \epsilon_c = 1.77$ for water, respectively. Two different sets of size parameters are calculated for the shell region composited by TiO_2 nanoparticles: (a, b) $a = \frac{\lambda}{30}$ and (c, d) $a = \frac{\lambda}{18}$.

$$V_n^{TM} \approx \frac{1}{(2n+1)^2}\left(\frac{k_c}{k_e}\right)^n\left(\frac{k_e}{k_s}\right)(k_e a)^{-2}\epsilon_s^{-2}\epsilon_e^{-1}\epsilon_c^{-1} \times \{n(n+1)\gamma^{2n}(\epsilon_e-\epsilon_s)(\epsilon_c-\epsilon_s) - \gamma^{-1}((n+1)\epsilon_e + n\epsilon_s)(n\epsilon_c + (n+1)\epsilon_s)\} \quad (9)$$

Here, we introduce the thickness ratio, $\gamma \equiv a_c/a$, which is defined as the ratio of inner core to whole particle radii. When $\gamma = 0$, the nanoparticle is fully filled (a solid-sphere), while when $\gamma = 1$, the nanoparticle is fully empty. A hollow sphere is described for $0 < \gamma < 1$.

For nonmagnetic materials, all the values of U_n^{TE} for different spherical harmonic channels are automatically zero. Thus, within this electrically small regime, the corresponding scattering coefficients for TE mode in every channel do not contribute to the scattering and absorption cross sections. On the other hand, in eq 2, the dominant term in the denominator of S_n^{TM} is now V_n^{TM}, with the leading term $(k_e a)^{-2}$. In this scenario, the corresponding cross sections in the electrically small limit become

$$Q_{abs} \sim Q_{ext} \approx \frac{4\pi}{|k_e|^2}(k_e a)^3 \times \mathrm{Im}\left[\frac{\gamma^3(2\epsilon_s+\epsilon_e)(\epsilon_s-\epsilon_c)+(\epsilon_e-\epsilon_s)(2\epsilon_s+\epsilon_c)}{2\gamma^3(\epsilon_e-\epsilon_s)(\epsilon_c-\epsilon_s)-(\epsilon_s+2\epsilon_e)(\epsilon_c+2\epsilon_s)}\right] \quad (10)$$

$$Q_{scat} \approx \frac{8\pi}{3|k_e|^2}(k_e a)^6\left|\frac{\gamma^3(2\epsilon_s+\epsilon_e)(\epsilon_s-\epsilon_c)+(\epsilon_e-\epsilon_s)(2\epsilon_s+\epsilon_c)}{2\gamma^3(\epsilon_e-\epsilon_s)(\epsilon_c-\epsilon_s)-(\epsilon_s+2\epsilon_e)(\epsilon_c+2\epsilon_s)}\right|^2 \quad (11)$$

Above results are also known as the dynamic dipole results, for one can obtain similar results by solving Laplace equation for an electrostatic dipole.

We want to remark that even in such an electrically small regime, one can have unusual optical properties by using composited meta-materials. Especially, with plasmonic materials, of which the real part of dielectric function is negative, enhancement in light scattering and absorption can happen due to the localized surface plasmonics.[24−29] Nevertheless, without the introduction of meta-materials, we show that counter-intuitive scattering and absorption properties exist for all dielectric materials in the shape of hollow spheres. If we apply the series expansion $\frac{1}{1-z} = \sum_{i=0}^{i=\infty} z^i$, for $|z| < 1$ by setting $z \equiv 2\gamma^3\frac{(\epsilon_e-\epsilon_s)^2}{(\epsilon_s+2\epsilon_e)(\epsilon_e+2\epsilon_s)}$, then the thickness effect on light absorption in the electrically small regime can be found explicitly:

$$Q_{abs} = \frac{4\pi}{|k_e|^2}(k_e a)^3\mathrm{Im}\left\{\frac{\epsilon_s-\epsilon_e}{\epsilon_s+2\epsilon_e}\frac{\gamma^3-1}{1-2\gamma^3\frac{(\epsilon_e-\epsilon_s)^2}{(\epsilon_s+2\epsilon_e)(\epsilon_e+2\epsilon_s)}}\right\} = \frac{4\pi}{|k_e|^2}(k_e a)^3\mathrm{Im}\left\{\frac{\epsilon_s-\epsilon_e}{\epsilon_s+2\epsilon_e} \times \left[\gamma^3 - 1 - 2\gamma^3\frac{(\epsilon_e-\epsilon_s)^2}{(\epsilon_s+2\epsilon_e)(\epsilon_e+2\epsilon_s)} + O(\gamma^6)\right]\right\} \quad (12)$$

From eq 12, one can see that the thickness, in terms of γ with the leading term to the cubic power, plays a minor role in light absorption. Based on this, we find that there exists a large range of thickness ratios to maintain nearly the same absorption cross section. As long as the ratio between inner core to whole particle radii is smaller than $\gamma = a_c/a \leq 0.4$, hollow spheres behave like the solid spheres, even with an empty core.

Analytical results based on eqs 10 and 11 are shown in Figure 3 for the absorption and scattering cross sections, Q_{abs} and Q_{scat}, with the dielectric constants $\epsilon_s = 7 + 0.1i$. It can be seen that the absorption cross section remains as a constant as long as the thickness ratio, $\gamma = a_c/a$, is smaller than 0.6. At the same time, the corresponding scattering cross section is not suppressed too much when $\gamma < 0.4$. However, when $\gamma > 0.4$, the scattering cross

DOI: 10.1021/acs.jpcc.5b08435
J. Phys. Chem. C 2015, 119, 25754−25760

section decreases to zero very quickly. Compared to numerical results conducted from exact solutions of Mie theory, shown in the dashed curves in Figure 3, our theoretical formulas based on the electrically small limit give the same tendency on the thickness effect. Even though a discrepancy arises when the thickness ratio γ approaches zero, it is due to the electrically small limit used. Nevertheless, we want to emphasize that this thickness-independent result can be applied to all composited systems, as long as off-resonance and electrically small conditions are satisfied.

Beyond Electrically Small Limit. The electrically small limit becomes invalid when the radius of TiO_2 nanoparticle is larger than 50 nm, that is, $k_s a \approx 1$. In this scenario, we can not approximate related spherical functions by a series of polynomial functions. To go beyond the electrically small limit, we look for the characteristic features in the original scattering spectrum for solid spheres. From Mie theory, it is well-known that interference between the incident and scattered fields occurs when the phase difference between them is fixed as a constant. As a result, the corresponding phase difference along the forward direction in a hollow sphere can be found as

$$\begin{aligned}\Delta\phi &= \frac{2\pi}{\lambda} \times 2\{\sqrt{\epsilon_s}(a - a_c) + \sqrt{\epsilon_e}a_c\} - \frac{2\pi}{\lambda} \times 2a\sqrt{\epsilon_e} \\ &= \frac{4\pi a}{\lambda}\{(\sqrt{\epsilon_s} - \sqrt{\epsilon_e}) - \gamma(\sqrt{\epsilon_s} - \sqrt{\epsilon_e})\} \\ &\equiv \text{const} \times a(1 - \gamma)\end{aligned} \tag{13}$$

where const stands for the constant related to the given material parameters. In eq 13, we reveal the relation between phase shift to particle radius a and thickness ratio γ. That is, there exists a trajectory for the constant scattering cross section in the phase space defined by the particle radius a and thickness ratio γ, and this trajectory can be described by $a(1 - \gamma) = \text{const}$, as shown in Figure 4.

Based on the exact solutions conducted from Mie theory, in Figure 4, we plot the values of normalized absorption and scattering cross sections $Q_{abs}/\pi a^2$ and $Q_{scat}/\pi a^2$ as a function of the particle size a (in unit of λ) and thickness ratio γ, for three different sets of dielectric constants for TiO_2 nanoparticles: (a, b) $\epsilon_s = 7 + 0.02i$, (c, d) $\epsilon_s = 8 + 0.1i$, and (e, f) $\epsilon_s = 9 + 0.3i$. As the dashed curves in white color shown in Figure 4b,d,e, the formula $a(1 - \gamma) = \text{const}$, shown in eq 13, can provide the role of thickness ratio on the scattering cross section for hollow spheres. Moreover, as shown in Figure 4a,c,e, the trajectories for a constant normalized absorption coefficient $Q_{abs}/\pi a^2$ can be represented in straight lines along the vertical direction. It means that when the thickness ratio γ is smaller than 0.4, the normalized absorption cross section is almost independent of the thickness ratio. For the normalized absorption cross section, one can see that its maximum value approaches to 1 when the imaginary part ϵ_s'' and outer radius a increase. However, this insensitive thickness effect survives for all three different sets of dielectric constants, as well as for different outer radii. It implies that we can have almost the same light absorption performance for a given particle radius, but with an additional degree of freedom in the thickness ratio.

EXPERIMENTS ON PHOTOCATALYTIC ACTIVITY

To verify our theoretical results for the absorption of nanoparticles in shape of hollow spheres, we perform

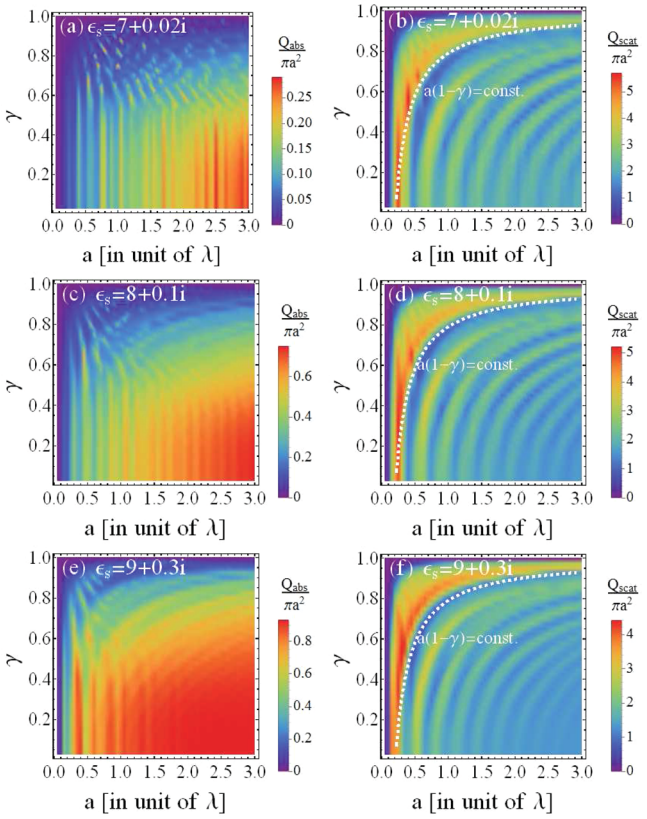

Figure 4. Normalized absorption and scattering cross sections $\frac{Q_{abs}}{\pi a^2}$ and $\frac{Q_{scat}}{\pi a^2}$ shown as a function of the particle size a (in unit of λ) and thickness ratio γ. Three different sets of dielectric constants for TiO_2 nanoparticles are used: (a, b) $\epsilon_s = 7 + 0.02i$, (c, d) $\epsilon_s = 8 + 0.1i$, and (e, f) $\epsilon_s = 9 + 0.3i$. The dashed curves in white color shown in the normalized scattering cross sections (b, d, e) are depicted from the formula $a(1 - \gamma) = \text{const}$, shown in eq 13.

experimentally the test of photocatalytic activity with the synthesized TiO_2 hollow spheres through the photodegradation of methylene blue. Here, uniform samples of hollow-sphere nanoparticles are tested with different radii, that is, but all with the same thickness in the shell region. By mixing 0.01 g of our TiO_2 nanoparticles with 50 mL of 25 ppm methylene blue solution, the solution is illuminated on top with a Xe bulb, from Osram Inc., operated at the output power 180 W and kept the temperature to 20 °C with a water cooling jacket. Samples of 0.5 mL are taken out every 5 min, filtered with a 0.2 μm filter, and diluted with 2 mL of deionized water. The filtrate is analyzed to determine the dye concentration, by a Hitachi UV-vis 3010 spectrophotometer.

Since the solution is dilute, we can safely assume that our photocatalytic behavior has a pseudo-first-order degradation rate constant, κ-value, which can be calculated by

$$\kappa = -\left[\ln\left(\frac{C}{C_0}\right)\right]/\Delta t \tag{14}$$

where C and C_0 are the corresponding final and initial concentrations of methylene blue, and Δt is the time period of interaction.

To have a comparison, same weight of hollow-sphere nanoparticles is performed under all the same conditions, but

DOI: 10.1021/acs.jpcc.5b08435
J. Phys. Chem. C 2015, 119, 25754−25760

with different particle radii. We want to emphasize that our hollow spheres are composed with the shells in 50 nm, which is much larger than that of the average migration length for the photon-generated carriers (holes and electrons). In this scenario, the effects from the migration to surface can also be ruled out. Experimentally measured data on these hollow spheres is shown in Figure 5, marked by Δ, for the degradation

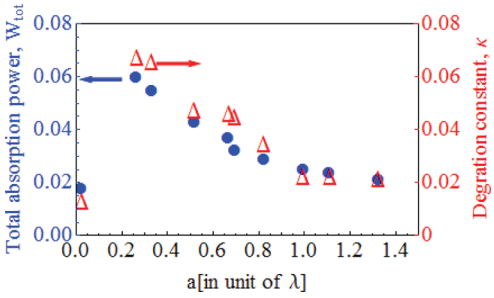

Figure 5. Total absorption power W_{tot} and related degradation constant κ for hollow-sphere nanoparticles in different particle radius, a (in unit of λ). Experimental hollow spheres have a thickness in the shell region about 50 nm, and λ = 388 nm is used as the incident light wavelength. Our measured particle radii differs from 94 to 500 nm. The Δ and ● markers correspond to the measured data points in the test of photocatalytic activity and theoretical calculations based on eq 15, respectively. A reference sample (on the left bottom side), made by crushing the original hollow-sphere particles into powders with the same weight, is also shown for the comparison, that is, $a = 0.02\lambda$. Here, the dielectric constant used is $\epsilon_s = 6.25 + 0.4i$.

constant κ. From Figure 5, one can see that the κ-value to measure photocatalytic activity is enhanced for hollow spheres when the particle radius is smaller than 250 nm, or equivalent γ = 0.8 or a = 0.644 in the unit of λ = 388 nm. Then, this value drops gradually from 0.05 to 0.02 as the radius increases to a = 0.9 (350 nm) or the thickness parameter γ = 0.9.

To link our experimental measurement on photocatalytic performance for hollow spheres, we take the weight of photoncatalyst into consideration. With the condition of same weight, we calculate the total absorption power of light for nanoparticles, W_{tot}, by including the total number of particles $N_{particle}$, that is,

$$W_{tot} = N_{particle} \times \frac{W_{abs}}{I_{inc}} \tag{15}$$

Here, due to its dynamic randomness and the dilute water solution, scattering from individual particles is assumed to be incoherent. Therefore, we can safely sum over all the total absorption power from each individual nanoparticle. For particles in shape of a fully filled solid-sphere, the total number of particles is $N_{particle}^{solid} = 3M/4\pi\rho a^3$, for a given mass M, the known material density ρ, and the particle radius a. But for particles in the shape of a hollow sphere, with the outer and inner radii defined as a and a_c, the corresponding total number of particles becomes $N_{particle}^{hollow} = 3M/4\pi\rho(a^3 - a_c^3)$. It can be understood that, for the same weight, we have more particle numbers in the shape of hollow spheres.

Numerical simulation of the total absorption power for hollow-sphere nanoparticles using the experimental conditions, W_{tot}, is also shown in Figure 5, marked by ● for different particle radii a in unit of λ. Again, a clear transition from high-absorption to low-absorption region can be seen as the particle radius increases. Our theoretical calculations based on eq 15 not only give good agreement to the experimental measurements on the photocatalytic activity, but also confirm the thickness effect of TiO_2 nanoparticles in the shape of hollow spheres. Moreover, a reference sample made by crushing the original hollow-sphere particles into powders with size of 10 nm, is also performed for the comparison. Here, for the measurements on crushed ones, the samples are prepared from a variety of hollow-sphere nanoparticles with different sizes. In each crushed samples, all of them reveal almost the same photocatalytic activity. In other words, the data is not taken from some specific hollow samples. The comparison to the crushed samples strongly supports our conclusion that the structural effect plays the dominant role upon photocatalytic activity. Experimental data from the measured degradation constant for this crushed sample is shown in Figure 5, too. Theoretical calculation by taking the particle radius as small as possible (taking a = 10 nm) also gives the same result for a smaller total absorption power.

By defining the parameter space through the particle size a (in unit of λ) and thickness ratio γ, in Figure 6 we show the

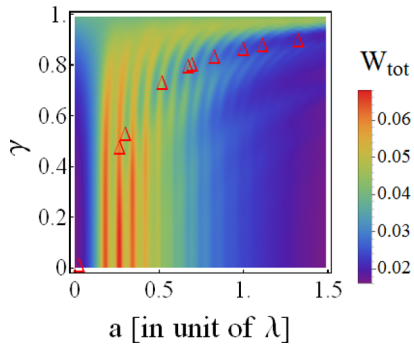

Figure 6. Same experimentally geometrical conditions as those shown in Figure 5, marked in Δ, are represented in the plot for the total absorption power, W_{tot}, as a function of the particle size a (in unit of λ) and thickness ratio γ.

total absorption power W_{tot} for different geometrical variables. In this diagram, several ways to achieve higher values in the total absorption power can be found with a suitable set of the size parameter and thickness ratio. As a comparison, the same experimental condition, in terms of (a,γ), from the photocatalytic activity shown in Figure 5 is also depicted in this diagram by using the same marker, Δ. Again, we can see that there are two groups for the data points: one for the hollow spheres located in the up-right quadrature, and the other one for crushed powders located near the origin. For the crushed powders, the corresponding total absorption power is pretty low $W_{tot} < 0.02$. But for the hollow spheres, one can see that all the data points with the particle size $a > 0.9$ have a low total absorption power $W_{tot} \sim 0.02$, while with the particle size $a < 0.8$, we have $W_{tot} \geq 0.04$. Moreover, there exists more delicate regions to support the total absorption power up to $W_{tot} = 0.07$. Based on this phase diagram, one can have an optimized absorption power for hollow-sphere nanoparticles by adjusting particle radius and its thickness.

CONCLUSION

In conclusion, we reveal the thickness effect on light absorption and scattering for nanoparticles in shape of hollow spheres theoretically and experimentally. Theoretically, based on the exact solution of Mie theory, we derive analytical formulas with

DOI: 10.1021/acs.jpcc.5b08435
J. Phys. Chem. C 2015, 119, 25754−25760

respect to the thickness ratio. Based on the theoretical formula, we find that, within and beyond the electrically small limits, one can maintain light absorption of hollow spheres to those of solid-spheres as long as the thickness ratio is smaller than 0.4. Moreover, with a different thickness parameter, we also reveal the possibility to have a higher total absorption power even with a larger particle size. Experimentally, we synthesize highly uniform hollow spheres of TiO_2 anatase through a self-sacrificing template method and perform related photocatalytic activity for light absorption. A variety of particle radii from 94 to 500 nm, with 50 nm in the shell thickness, are tested and give a good agreement with our theoretical results. With experimental demonstrations and theoretical simulations, these nanoparticles in the shape of hollow spheres would serve as the platform for green energy applications from light harvesting, solar cell, and water splitting to CO_2 reduction.

AUTHOR INFORMATION

Corresponding Author

*E-mail: rklee@ee.nthu.edu.tw.

Notes

The authors declare no competing financial interest.

ACKNOWLEDGMENTS

The research was supported by the National Center for Theoretical Science and the Ministry of Science and Technology in Taiwan.

REFERENCES

(1) Fujishima, A.; Honda, K. Electrochemical Photolysis of Water at a Semiconductor Electrode. *Nature* **1972**, *238*, 37−38.

(2) Chen, X.; Shen, S.; Guo, L.; Mao, S. S. Semiconductor-Based Photocatalytic Hydrogen Generation. *Chem. Rev.* **2010**, *110*, 6503−6570.

(3) Hashimoto, K.; Irie, H.; Fujishima, A. TiO_2 Photocatalysis: a Historical Overview and Future Prospects. *Jpn. J. Appl. Phys.* **2005**, *44*, 8269.

(4) Nakata, K.; Fujishima, A. TiO_2 Photocatalysis: Design and Applications. *J. Photochem. Photobiol., C* **2012**, *13*, 169−189.

(5) Kamat, P. V. TiO_2 Nanostructures: Recent Physical Chemistry Advances. *J. Phys. Chem. C* **2012**, *116*, 11849−11851.

(6) Hurum, D. C.; Gray, K. A.; Rajh, T.; Thurnauer, M. C. Recombination Pathways in the Degussa P25 Formulation of TiO_2: Surface versus Lattice Mechanisms. *J. Phys. Chem. B* **2005**, *109*, 977−980.

(7) Yu, J. G.; Xiong, J. F.; Cheng, B.; Liu, S. W. Fabrication and Characterization of *Ag-*TiO_2 Multiphase Nanocomposite Thin Films with Enhanced Photocatalytic Activity. *Appl. Catal., B* **2005**, *60*, 211−221.

(8) Li, G. H.; Gray, K. A. The Solid-Solid Interface: Explaining the High and Unique Photocatalytic Reactivity of TiO_2-Based Nanocomposite Materials. *Chem. Phys.* **2007**, *339*, 173−187.

(9) Irie, H.; Watanabe, Y.; Hashimoto, K. Carbon-Doped Anatase TiO_2 Powders as a Visible-Light Sensitive Photocatalyst. *Chem. Lett.* **2003**, *32*, 772−773.

(10) Ohno, T.; Akiyoshi, M.; Umebayashi, T.; Asai, K.; Mitsui, T. Preparation of S-Doped TiO_2 Photocatalysts and Their Photocatalytic Activities under Visible Light. *Appl. Catal., A* **2004**, *265*, 115−121.

(11) Asahi, R.; Morikawa, T.; Ohwaki, T.; Aoki, K.; Taqa, Y. Visible Light Photocatalysis in Nitrogen-Doped Titanium Oxides. *Science* **2001**, *293*, 269−271.

(12) Zhu, W.; Qiu, X.; Iancu, V.; Chen, X.; Pan, H.; Wang, W.; Dimitrijevic, N. M.; Rajh, T.; Meyer, H. M.; Paranthaman, M. P.; et al. Band Gap Narrowing of Titanium Oxide Semiconductors by Noncompensated Anion-Cation Codoping for Enhanced Visible-Light Photoactivity. *Phys. Rev. Lett.* **2009**, *103*, 226401.

(13) Zhang, X.; Chen, Y. L.; Liu, R.-S.; Tsai, D. P. Plasmonic Photocatalysis. *Rep. Prog. Phys.* **2013**, *76*, 046401.

(14) Chen, J.-J.; Wu, J. C. S.; Wu, P. C.; Tsai, D. P. Plasmonic Photocatalyst for H_2 Evolution in Photocatalytic Water Splitting. *J. Phys. Chem. C* **2011**, *115*, 210−216.

(15) Li, H.; Bian, Z.; Zhu, J.; Zhang, D.; Li, G.; Huo, Y.; Li, H.; Lu, Y. Mesoporous Titania Spheres with Tunable Chamber Structure and Enhanced Photocatalytic Activity. *J. Am. Chem. Soc.* **2007**, *129*, 8406−8407.

(16) Xu, H.; Chen, X.; Ouyang, S.; Kako, T.; Ye, J. Size-Dependent Mie's Scattering Effect on TiO_2 Spheres for the Superior Photoactivity of H_2 Evolution. *J. Phys. Chem. C* **2012**, *116*, 3833−3839.

(17) Tsai, M.-C.; Lee, J.-Y.; Chen, P. C.; Chang, Y. W.; Chang, Y.-C.; Yang, M.-H.; Chiu, H.-T.; Lin, I. N.; Lee, R.-K.; Lee, C.-Y. Effects of Size and Shell Thickness of TiO_2 Hierarchical Hollow Spheres on Photocatalytic Behavior: an Experimental and Theoretical Study. *Appl. Catal., B* **2014**, *147*, 499−507.

(18) Tsai, M.-C.; Lee, J.-Y.; Chang, Y.-C.; Yang, M.-H.; Chen, T.-T.; Chang, I.-C.; Lee, P.-C.; Chiu, H.-T.; Lee, R.-K.; Lee, C.-Y. Scattering Resonance Enhanced Dye Absorption of Dye Sensitized Solar Cells at Optimized Hollow Structure Size. *J. Power Sources* **2014**, *268*, 1−6.

(19) Zhou, H.; Fan, T.; Ding, J.; Zhang, D.; Guo, Q. Bacteria-Directed Construction of Hollow TiO_2 Micro/Nanostructures with Enhanced Photocatalytic Hydrogen Evolution Activity. *Opt. Express* **2012**, *20*, 340−350.

(20) Bohren, C. F.; Huffman, D. R. *Absorption and Scattering of Light by Small Particles*; John Wily & Sons: New York, 1983.

(21) Wu, G. S.; Wang, J. P.; Thomas, D. F.; Chen, A. C. Synthesis of F-doped Flower-Like TiO_2 Nanostructures with High Photoelectrochemical Activity. *Langmuir* **2008**, *24*, 3503−3509.

(22) Asahi, R.; Taqa, Y.; Mannstadt, W.; Freeman, A. J. Electronic and Optical Properties of Anatase TiO_2. *Phys. Rev. B: Condens. Matter Mater. Phys.* **2000**, *61*, 7459−7465.

(23) Landmann, M.; Rauls, E.; Schmidt, W. G. The Electronic Structure and Optical Response of Rutile, Anatase and Brookite TiO_2. *J. Phys.: Condens. Matter* **2012**, *24*, 195503.

(24) Alú, A.; Engheta, N. Polarizabilities and Effective Parameters for Collections of Spherical Nanoparticles Formed by Pairs of Concentric Double-Negative, Single-Negative, and/or Double-Positive Metamaterial Layers. *J. Appl. Phys.* **2005**, *97*, 094310.

(25) Alú, A.; Engheta, N. Achieving Transparency with Plasmonic and Metamaterial Coatings. *Phys. Rev. E* **2005**, *72*, 016623.

(26) Ruan, Z.; Fan, S. Superscattering of Light from Subwavelength Nanostructures. *Phys. Rev. Lett.* **2010**, *105*, 013901.

(27) Tribelsky, M. I. Anomalous Light Absorption by Small Particles. *Europhys. Lett.* **2011**, *94*, 14004.

(28) Tribelsky, M. I.; Lukyanchuk, B. S. Anomalous Light Scattering by Small Particles. *Phys. Rev. Lett.* **2006**, *97*, 263902.

(29) Cao, L. Y.; Fan, P. Y.; Vasudev, A. P.; White, J. S.; Yu, Z.; Cai, W.; Schuller, J. A.; Fan, S.; Brongersma, M. L. Semiconductor Nanowire Optical Antenna Solar Absorbers. *Nano Lett.* **2010**, *10*, 439.

DOI: 10.1021/acs.jpcc.5b08435
J. Phys. Chem. C 2015, 119, 25754−25760